euspen's 20th International Conference & Exhibition, Geneva, CH, June 2020
www.euspen.eu

Simulation and experimental study on the effect of interelectrode gap on the cavities machined by hybrid laser-electrochemical micromachining process

Krishna Kumar Saxena[1,3], Xiaolei Chen[1,2], Jun Qian[1,3], Dominiek Reynaerts[1,3]

[1]*Manufacturing Processes and Systems (MaPS), Department of Mechanical Engineering, KU Leuven, Leuven, Belgium.*
[2]*School of Electromechanical Engineering, Guangdong University of Technology, Guangzhou, 510016, PR China.*
[3]*Member Flanders Make, Leuven, Belgium.*

dominiek.reynaerts@kuleuven.be

Abstract
The term hybrid machining refers to the use of two or more process energies simultaneously in the same machining zone so as to exploit additional benefits from their interaction. Hybrid laser-electrochemical micromachining process involves laser and electrochemical processes applied concurrently in the same machining zone. The process derives additional advantages from the interaction of the two process energies in the same machining zone. To enable the simultaneous application of laser and ECM in the same machining zone, a hybrid tool concept is used where the tools serves the function of both an ECM tool and a multimode waveguide for the laser. This paper presents the simulation and experimental investigations on the effect of interelectrode gap on the profiles of the cavities machined by hybrid laser-electrochemical micromachining process. Experimental investigations are performed on Inconel IN718 as workpiece material. The results have been explained by means of multiphysics ECM simulations. Overall, it is shown that interelectrode gap is an important parameter influencing the machining response in the current configuration of hybrid process.

Keywords: Hybrid machining, Non-conventional machining , ECM, Electrochemical machining, Laser-electrochemical machining.

1. Introduction

Electrochemical micromachining [1] has evolved as a promising machining technology for fabricating complex, high surface quality and defect-free shapes on difficult-to-cut materials without affecting mechanical, functional or microstructural property of workpiece material. The technology has passed through several research phases including process development, tooling/machine-tool development, process-material interaction, electrolyte development and methods to improve process accuracy [2]. Electrochemical machining has several interesting properties such as the non-contact nature of the process, independent of workpiece hardness, and no process-related tool wear. This makes ECM a good candidate for hybridization with other processes. One promising hybridization of ECM is hybrid laser-ECM process where the two processes (i.e. ECM and laser) can either participate simultaneously in material removal or assist each other. In prior state of the art [3], [4]; it has been proposed that hybrid laser-ECM process offers gentle material processing, weakening of passivation layer, accelerated material removal due to temperature induced increase in reaction kinetics, reduced heat affected zone and spatter in case of laser as main process energy and more uniform dissolution of multi-phase materials. The present research focusses on a tool based hybrid laser-electrochemical micromachining technology [5] where the tool serves dual function of an ECM tool and a multimode waveguide for the laser.

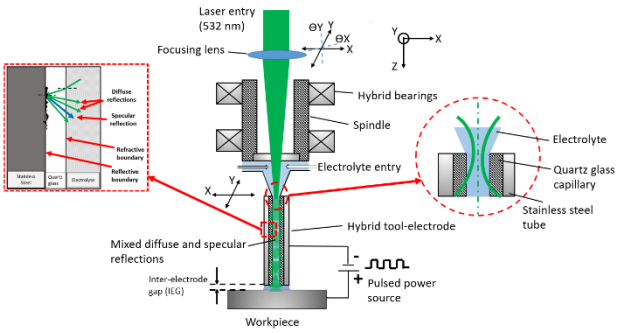

Figure 1. Process schematic of a tool based hybrid laser-electrochemical micromachining process.

The interelectrode gap (IEG) is an important parameter which influences machining efficiency, workpiece surface quality, shape precision, temperature distribution and current density distribution during hybrid laser-electrochemical micromachining process. In this work, combination of simulation and experiments is used to study the effect of interelectrode gap on the process performance.

2. Simulation and results

In order to study the effect of interelectrode gap, a multiphysics model (Figure 2) is developed in Comsol 5.4® considering primary electric currents, fluid dynamics and heat transfer physics. The electrolyte flow is modelled using the k-epsilon turbulence model in Comsol 5.4®. The tool is a hybrid tool which comprises an outer layer of stainless-steel (EN 1.4301) tube and an inner concentric layer of quartz glass. The workpiece is Inconel IN718. The electrolyte is 200 *g/l aq.* $NaNO_3$ with electrical conductivity of 12 S/m. The two-phase electrical conductivity is modelled using Eq. *(i)*. A property switch is created in the software based on temperature threshold. The liquid phase electrical conducitivity is described using Eq. *(ii)*. The vapor phase electrical conducitivity should be ideally zero. However, to improve convergence and avoid sharp transition of electrical conductivity to zero, a mathematical function is

defined as in Eq. *(iii)*. This model only takes into account the laser induced temperature effects and doesn't takes into account the temperature effects on reaction kinetics.

$$\rho = \begin{cases} \rho\_el(T) & (if\ T \leq 393\ K) \\ \rho\_vap(T) & (if\ T > 393\ K) \end{cases} \qquad (i)$$

$$\rho_{el(T)} = \rho_E(1-\beta)^{\frac{3}{2}}\left(1+\alpha(T-T_{ambient})\right) \qquad (ii)$$

$$\rho\_vap(T) = \frac{\rho\_el_{T=393\ K}}{e^{\frac{T-393}{100}}} \qquad (iii)$$

The laser source is applied as a Gaussian heat flux on the workpiece surface and is modelled using Eq. *(iv)*

$$Q(r)|\Gamma_1 = \frac{P_a}{\pi R^2}.(1-R_{el}).\alpha_{IN}.exp\left(\frac{-2r^2}{R^2}\right) \qquad (iv)$$

The model parameters are depicted in Table 1. The temperature (T) and electrical conductivity (ρ) are evaluated at the workpiece surface (T_0, ρ_0) as well as along the section line XX (Figure 2) passing through the centre of inter-electrode gap (T_1, ρ_1).

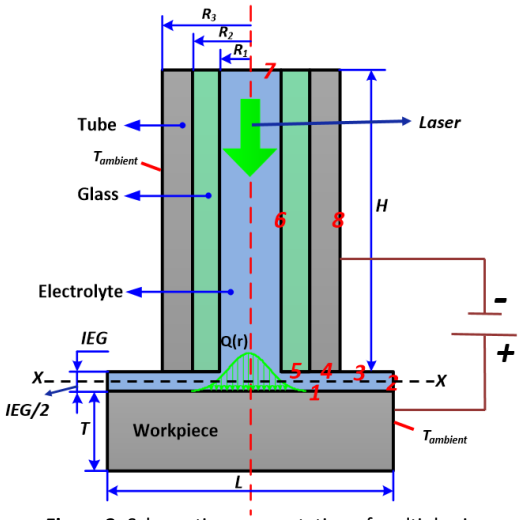

Figure 2. Schematic representation of multiphysics model of hybrid laser-ECM process.

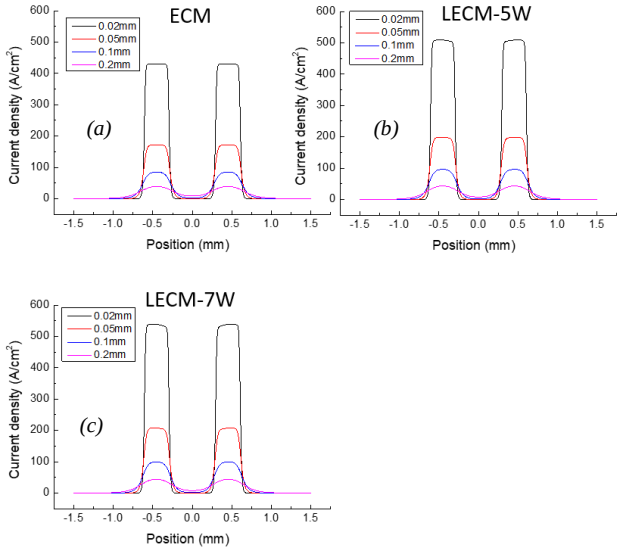

Figure 3. Current density distribution on the workpiece surface at different IEG values for (a) ECM process (b) laser-ECM process with average laser power 5 W and (c) laser-ECM process with average laser power 7 W.

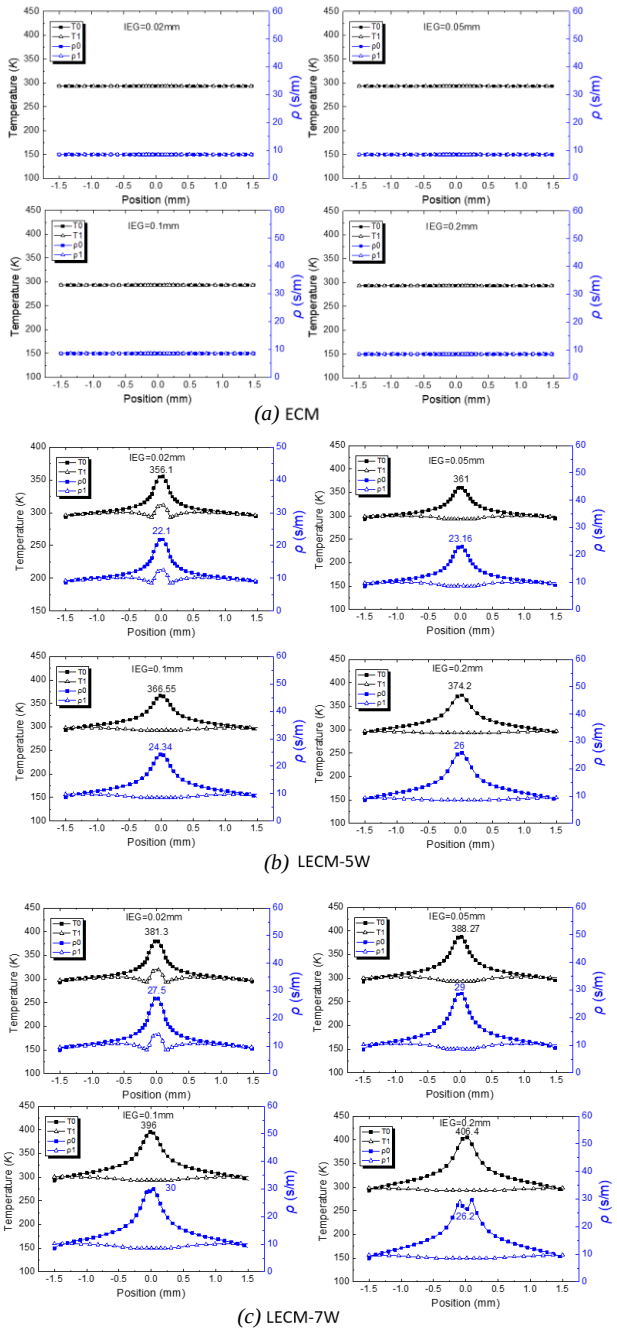

Figure 4. Temperature and electrical conductivity profiles for (a) ECM process (b) Laser-ECM with average laser power of 5 W (c) Laser-ECM with average laser power of 7 W for different IEG values i.e. 20, 50, 100 , 200 µm.

Table 1. Model parameters.

Model parameter	Value
Electrolyte conductivity, ρ_E	12 (S/m)
Gas volume fraction, β	0.2 (assumed)
Coefficient of thermal exp., α	0.025 (1/K)
Ambient temperature, $T_{ambient}$	293.15 K
Reflectivity of electrolyte *(Rel)*	0.04 @532 nm
Absorptivity of Inconel (α_{IN})	0.5 @532 nm
Laser average power (P_a)	5, 7 W
Voltage	20 V
Interelectrode gap (IEG)	20, 50, 100, 200 µm

Figure 3 shows the electric current density distribution for ECM and laser-ECM process at different IEGs. IEG values below 20 µm were not simulated as they are more prone to short-circuits based on experimental experience with the process. For the ECM process (Figure 3(a)), it is clear that at shorter IEGs, the impedance of the gap is lower and hence higher current densities are observed on the workpiece. It can be seen from Fig. 3(a) that the maximum current density at IEG = 20 µm is more than 2.5 times the maximum current density at IEG = 200 µm. It can be observed from Figure 3(b&c) that for laser-ECM process, the temperature effects come into picture and a slight temperature induced rise in current density is observed. This model does not takes into account the reaction kinetics so only the effect of temperature on the primary currents is seen. For this laser-ECM process, it can be observed that the current density is higher at shorter IEGs (20, 50 µm) as compared to higher IEGs (100, 200 µm). At higher IEGs, the current density values in laser-ECM are nearly the same as in ECM process. This can be explained on the basis of the fact that at higher IEGs, the convection effects are dominant as the flow conditions improve due to increase in IEG. As a result, the temperature accumulation is less pronounced and current density is nearly the same as in ECM process. Furthermore, it can also be observed that at average laser power of 7 W, the temperature induced rise in current density effect does not improves a lot as the power is increased from 5 to 7 W. This can be due to the reason that at 7 W laser power, electrolyte phase change (liquid to vapor) starts occurring and hence the electrical conductivity drops which limits rise in current density corresponding to the laser power applied. These results will be further correlated with the temperature and electrical conductivity profiles as in Figure 4.

Figure 4(a-c) shows the temperature and electrical conductivity variation for different IEGs for ECM and laser-ECM process. The temperature and electrical conductivity are evaluated at two different positions, one on the workpiece surface (T_0, ρ_0) and other along the section line XX (Figure 2) along the centre of IEG (T_1, ρ_1). It can be observed from Figure 4(a), that the temperature and electrical conductivity remains nearly unchanged with a change in IEG. This is also independent of the location. There is no change in the simulated temperature and electrical conductivity along the workpiece surface and along the line XX. It can be observed from Figure 4(b) that during the laser-ECM process, the temperature is higher below the tool in the centre of workpiece. At 5W laser power and considering a turbulent flow model, a temperature of about 356 K is observed at an IEG of 20 µm. When the IEG is increased to 50 µm, there is a 5 K rise in the temperature when IEG is increased from 20 to 50 µm. The magnitude of temperature is maximum at IEG 200 µm. It can also be observed that there is not a drastic change in temperature (T_0) or electrical conductivity (ρ_0) along the line XX. This is because the electrolyte is continuously flushed and there is no accumulation of thermal energy. A similar trend is observed for the laser-ECM process at a laser average power of 7 W as in Figure 4(c). At IEG of 200 µm (Fig. 4(c)), maximum temperature is observed which also causes evaporation of small packets of electrolytes and the electrical conductivity drops. The increase in temperature with an increase in IEG on the workpiece surface can be explained on the basis of two phenomena (i) An increase in IEG leads to a decrease in flow velocity and results in temperature accumulation in the centre and therefore temperatures are higher at higher IEGs. This can be observed in Figure 5 where the velocity magnitudes are shown for different IEG values. (ii) A reduction in IEG leads to some fraction of heat being conducted back into the tool and thus less heat is available for the workpiece. With an increase in IEG, a larger fraction of heat is available on the workpiece. The effects of temperature in the centre are not seen completely on the current density profiles in Figure 3 because the model considers only primary currents. To account for the temperature effects on diffusion of species/charge transfer/mass transport, secondary and tertiary currents need to be included in the simulation which is beyond the scope of this paper.

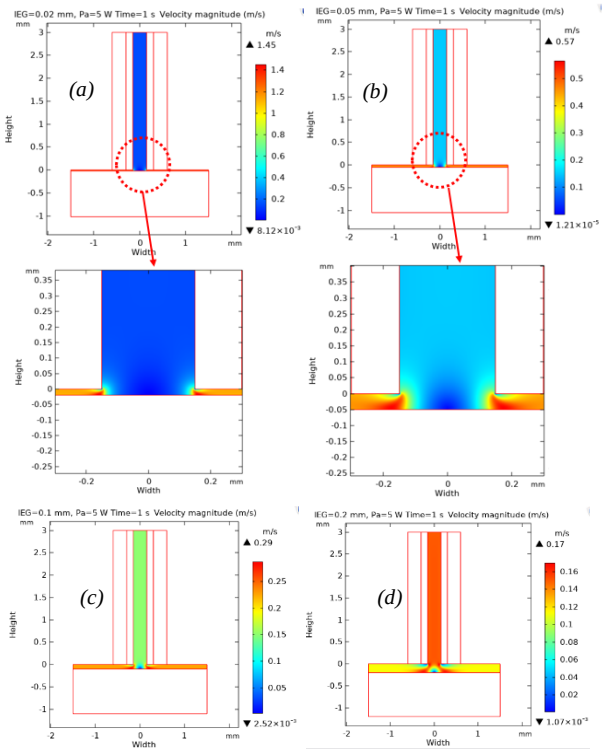

Figure 5. Variation of electrolyte velocity in the inter-electrode gap for different IEGs.

3. Experimentation and results

To study the effect of IEG on the machined cavities, a limited set of experiments has been conducted. An in-house developed prototype hybrid laser-ECM machine tool was used for experiments (as in Figure 6) [6]. A ns pulsed green laser of 532 nm wavelength was used as it has negligible absorption in water. The equipment is controlled using NI® Crio system as master controller and the controllers of other peripherals were slave controllers. Table 2 shows experimental parameters. The three dimensional profiles of machined cavities were acquired using Sensofar® Neox microscope in confocal mode.

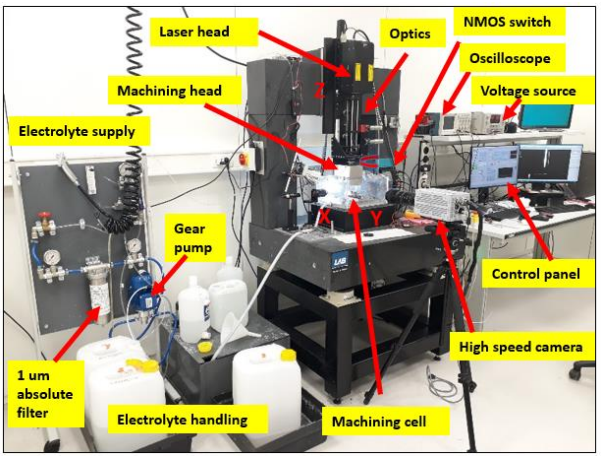

Figure 6. Prorotype hybrid laser-ECM machine tool with major peripherals.

Table 2. Experimental parameters.

Experimental parameter	Value
Electrolyte	200 *g/l aq.* $NaNO_3$
Electrolyte conductivity (measured)	12.9 S/m @ 19.3 ^{0}C
Workpiece material	Inconel IN718
Voltage	20 V
ECM pulse on time and duty cycle	10 µs, 50 %
Laser average power (P_a)	5, 7 W
Laser wavelength	532 nm
Laser pulse on time and repetition rate	50 ns, 150 kHz
Interelectrode gap (IEG)	20, 50 µm
Machining time	20 s

Figure 7 shows the cavity profiles machined at IEGs of 20 and 50 µm using ECM and laser ECM with laser average power of 5W and 7W. It can be observed that for ECM process, there exists a central undissolved pin for IEG of 20 µm whereas at IEG of 50 µm, the pin is dissolved with a very little undissolved feature left in the centre. This is because at IEG of 50 µm, the current transfer occurs via the electrolyte jet similar to the jet-ECM technology. At IEG of 20 µm, the current density is highest and localized mainly below the conductive area of tool and in the centre the current densities are not sufficient to cause dissolution. In case of the laser-ECM process, the central feature is dissolved due to a temperature induced rise in the electrical conductivity of the electrolyte as explained in the simulation section. Furthermore, the dissolution area in the centre (blue color in Fig. 7) starts to become larger when the IEG is changed from 20 to 50 µm for laser-ECM process at both average laser powers of 5 and 7 W. This can be explained on the basis of simulated temperature and flow field as in Fig. 4 and 5. This is because at an IEG of 50 µm the temperature is relatively higher because of lower flow velocity in the gap. Thus, the temperature induced interaction between laser and ECM is more pronounced. There are additional temperature effects on reaction kinetics and mass transport which have not been considered in the model in this paper. Additionally, the dimensional accuracy is better at an IEG of 20 µm and the edges are well defined (sharp) as compared to the cavities at IEG of 50 µm.

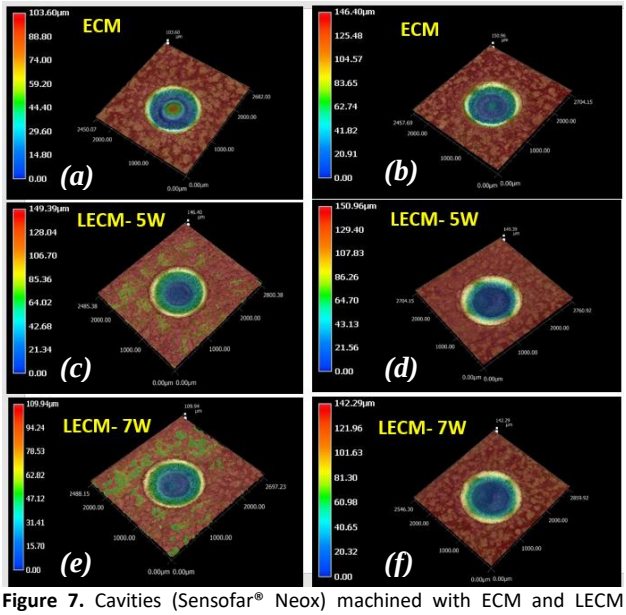

Figure 7. Cavities (Sensofar® Neox) machined with ECM and LECM process at different IEGs. (a,c,e) IEG = 20 µm (b,d,f) IEG = 50 µm.

4. Conclusions

In this work, simulation and experimental investigations were carried out to study the effect of interelectrode gap on the machined cavities during hybrid laser-ECM process. The following points can be concluded:

(i) It is already known for ECM process that with an increase in IEG, the gap reactance increases and the current density decreases. Similar current density trends are observed for laser-ECM process as well. However the current densities with laser-ECM process are a bit higher due to a temperature induced rise in electrolyte conductivity. At IEG of 20 µm, an 18.6 % and 25.5 % rise in maximum current density is observed from ECM to laser-ECM 5W and laser-ECM 7W respectively. On the other hand at higher IEG of 200 µm, the maximum current densities rise only about 7.5 % and 12.5 % respectively for ECM to laser-ECM 5W and laser-ECM 7 W. This is based on model prediction considering primary currents only. Temperature induced reaction kinetics and diffusion/mass transport effects are not considered here.

(ii) Based on the combined thermal and flow field simulations, it can be concluded that the workpiece surface temperature is higher at higher IEGs due to decrease in flow velocity in the gap. Furthermore, at small IEGs, some part of the heat is conducted back into the tool.

(iii) From the experimental investigations, it can be observed that the dimensional accuracy is higher at smaller IEGs. The edge of the cavities become sharper as the IEG is decreased. From the experimental experience, IEGs of 10 µm or below are not desired as they cause repetitive short circuits and the process becomes unstable.

Overall it can be concluded that the setting of interelectrode gap (IEG) is a crticial decision in the laser-ECM process. This is because this hybrid process deals with both electrical and thermal fields. It is desired not only to have small IEGs for better dimensional accuracy but also to have a stable process with desired current densities, no short-circuits, better flushing of by-products and better temperature control in hybrid laser-ECM process.

Acknowledgements

This research work was undertaken in the context of Marie Curie ITN project MICROMAN (GA# 674801) and European FoF project PROSURF (GA# 767589). It is also partially sponsored by Flanders Make vzw – exploratory research allocation.

References

[1] R. Schuster, V. Kirchner, P. Allongue, and G. Ertl, "Electrochemical micromachining," *Science (80-.).*, vol. 289, no. 5476, pp. 98–101, 2000.

[2] K. K. Saxena, J. Qian, and D. Reynaerts, "A review on process capabilities of electrochemical micromachining and its hybrid variants," *Int. J. Mach. Tools Manuf.*, vol. 127, pp. 28–56, 2018.

[3] P. T. Pajak, A. K. M. Desilva, D. K. Harrison, and J. A. Mcgeough, "Precision and efficiency of laser assisted jet electrochemical machining," *Precis. Eng.*, vol. 30, pp. 288–298, 2006.

[4] A. Stephen and F. Vollertsen, "Mechanisms and processing limits in laser thermochemical machining," *CIRP Ann. - Manuf. Technol.*, vol. 59, no. 1, pp. 251–254, 2010.

[5] K. K. Saxena, J. Qian, and D. Reynaerts, "Research on hybrid laser-electrochemical micromachining: Prototype machine-tool development and test machining results (Session keynote)," in *euspen 19th International Conference and Exhibition, Bilbao, Spain. ISBN: 978-0-9957751-4-5*, 2019, pp. 476–479.